

Mantle redox in Cordilleran ophiolites as a record of oxygen fugacity during partial melting and the lifetime of mantle lithosphere

Dante Canil^{a,*}, Stephen T. Johnston^a, Mitchell Mihalynuk^b

^a School of Earth and Ocean Sciences, University of Victoria, 3800 Finnerty Rd., Victoria BC V8W 3P6 Canada

^b Geological Survey, British Columbia Ministry of Energy and Mines, Victoria, B.C., Canada

Received 2 November 2005; received in revised form 18 April 2006; accepted 24 April 2006

Available online 27 June 2006

Editor: R.W. Carlson

Abstract

We examine controls on mantle oxygen fugacity (fO_2) during the partial melting process that forms mantle lithosphere at spreading centers. We compare the paleo fO_2 at the time of melting inferred by V/Sc systematics of ophiolite peridotites, with the thermobarometric fO_2 recorded by olivine–orthopyroxene–spinel assemblages during simple cooling in relatively young oceanic lithosphere. Modelling of the V/Sc in the ophiolite peridotites from Alaska, Yukon and British Columbia is permissive of only a narrow range in $\log fO_2$ during melting between NNO and NNO – 1 (where NNO is the nickel–nickel oxide buffer), depending on the choice of partition coefficients for Sc. This result is within uncertainty of the thermobarometric fO_2 recorded by most samples (within 1 log unit of NNO – 1). The same cannot be said for more complex peridotite residues from continental mantle, where V/Sc systematics show a narrow paleo fO_2 during formation but wide range of thermobarometric fO_2 after equilibration in the lithosphere. In continental mantle with a complex history, thermobarometric fO_2 is an ambiguous measure of that attendant during partial melting. Graphite-saturated melting in a system closed to oxygen controls melt Fe^{3+}/Fe^{2+} and CO_2 content, and creates a shift in fO_2 of about 2 log units [1] in a peridotite residue. In contrast, for the ophiolite mantle samples in this study, both paleo- and thermobarometric fO_2 are near values predicted by carbon–fluid equilibria, yet show no relationship with depletion, suggesting the melt–residue system in the mantle may be open to oxygen during the partial melting process.

© 2006 Elsevier B.V. All rights reserved.

Keywords: mantle; redox; oxygen; melting; ophiolite; peridotite; Cordillera

1. Introduction

Decades of study of mantle oxygen fugacity (fO_2) have been motivated by several far-reaching implications of this intensive variable. For example, fO_2 dictates the form of sequestration of carbon in the mantle [2] and its dissolution into magmas which degas in the exosphere, governing the geochemical cycle of atmophile elements

[1]. The stability of sulfides and sequestration of chalcophile or siderophile elements from the mantle to produce prodigious ore deposits may also be controlled by mantle fO_2 [3]. The origin of oxygen in the earth's atmosphere, a key element in weathering cycles and the evolution of complex life forms, is tied to the history of mantle degassing, dictated by mantle redox state over time [4,5].

Despite extensive study, however, overarching questions remain as to what changes mantle fO_2 and how well buffered the mantle system is and by what mechanisms. Contrasting views abound from different datasets [6–11].

* Corresponding author.

E-mail address: dcanil@uvic.ca (D. Canil).

This stems partly from the fact that many studies base their estimate of mantle fO_2 on that recorded as an intensive variable determined ‘thermobarometrically’ using mineral assemblages of mantle-derived rocks exhumed to the surface. Thermobarometric fO_2 for mantle samples from several settings varies by $\sim 5 \log fO_2$ units. In contrast, extensive variables (e.g. bulk composition), based on the partitioning of V or Cr between mantle minerals and melts, have been used as a proxy for the ‘paleo- fO_2 ’ at the time a residue originally formed, in order to see through the subsequent complex (billion year) history of mantle samples [12,13]. The paleo- fO_2 approach, though not in itself intended as a test of thermobarometric methods, shows a narrow range, and little if any change in mantle fO_2 for the past 4 Ga [12–15]. A refinement of the latter approach uses the observation that V and Sc have similar partitioning behaviour between melts and residues during melting, except that the former is sensitive to fO_2 , thus making the V/Sc ratio a more precise measure of the paleo- fO_2 for a melt or residue. The V/Sc of residues records an even more restricted range of paleo- fO_2 (within 1 log unit) for mantle melts and residues [16,17]. The question thus remains: Does thermobarometric fO_2 of mantle samples represent a different and varied signal compared to the paleo- fO_2 when the residues first formed, and if so how and why does this difference come about? In addition, what would such a difference tell us about the behaviour of oxygen in the mantle during partial melting?

A second important factor obscuring the discussion on the controls of fO_2 are the differences between oceanic and continental mantle. The oceanic lithospheric mantle, represented by abyssal peridotites and ophiolites, has a comparatively simple history, being produced by melt extraction at spreading centers and cooled. In the case of ophiolites, the lithosphere is obducted within only tens of million years of its formation [18]. In contrast, continental mantle sampled as xenoliths or in massifs has a billion year history during which it interacts with melts rising into the continental plates [19,20]. The vast majority of studies concerning mantle fO_2 are based on thermobarometric data for continental mantle samples with this protracted history.

In this paper, we examine what controls mantle oxygen fugacity during the production and history of mantle lithosphere formed at spreading centers and having a simple cooling history. To achieve this goal, we examine and compare the paleo- fO_2 at the time of melting recorded by the V/Sc systematics of peridotites with the thermobarometric fO_2 as recorded by mineral equilibria. Our results derive from a dataset of ophiolite peridotites from several regions in the northern Cordillera of Alaska, Yukon and British Columbia, which were sampled at

different spatial scales. Although most ophiolites are interpreted to have been related to convergent margin tectonic settings, their lithosphere is interpreted to have formed by the seafloor spreading process [18]. Thus, we chose to examine ophiolite peridotite samples for our purpose because of their simple history, compared to continental mantle, allowing us to understand what controls fO_2 during the partial melting process, and during the subsequent cooling and emplacement of mantle lithosphere. Our investigation allows us to address the fundamental issue of whether oxygen behaves in an open or closed system during partial melting.

2. Samples and geologic setting

Ophiolites throughout the North American Cordillera have been the subject of detailed studies in California and Oregon (see [21], but with fewer detailed studies in northern British Columbia, Yukon and Alaska. Samples for this study derive from well-exposed ophiolites in the northern Cordillera (Fig. 1) which are part of recent comprehensive field studies [22–25].

2.1. Cascaden Ridge/Livengood

Two elongated ultramafic massifs exposed ~ 100 km north of Fairbanks, Alaska are included in a Devonian ultramafic–clastic complex in the Livengood terrane [26].

2.2. American Creek

Well-preserved peridotite in a ~ 25 km² massif is exposed along American Creek in east–central Alaska [22] and is included in ophiolite of the Permian Seventy Mile/Slide Mountain terrane in Alaska and Yukon [27].

2.3. Harzburgite Peak

An imbricated sequence of gabbros, sheeted dikes and spinel harzburgite together with regional aeromagnetic patterns are interpreted as parts of an ophiolite with a strike length extending ~ 100 km throughout southwest Yukon [23]. Well-preserved, coarse-textured harzburgite tectonite is exposed over ~ 75 km². The ophiolite is intruded by mid-Cretaceous plutons, and is older than the Mississippian strata present in its footwall.

2.4. Lake Laberge

Dark green, fuchoidal, talc-serpentine schist is exposed for 4 km along southern Lake Laberge, Yukon [28]. The schist contains knockers and augen of undeformed

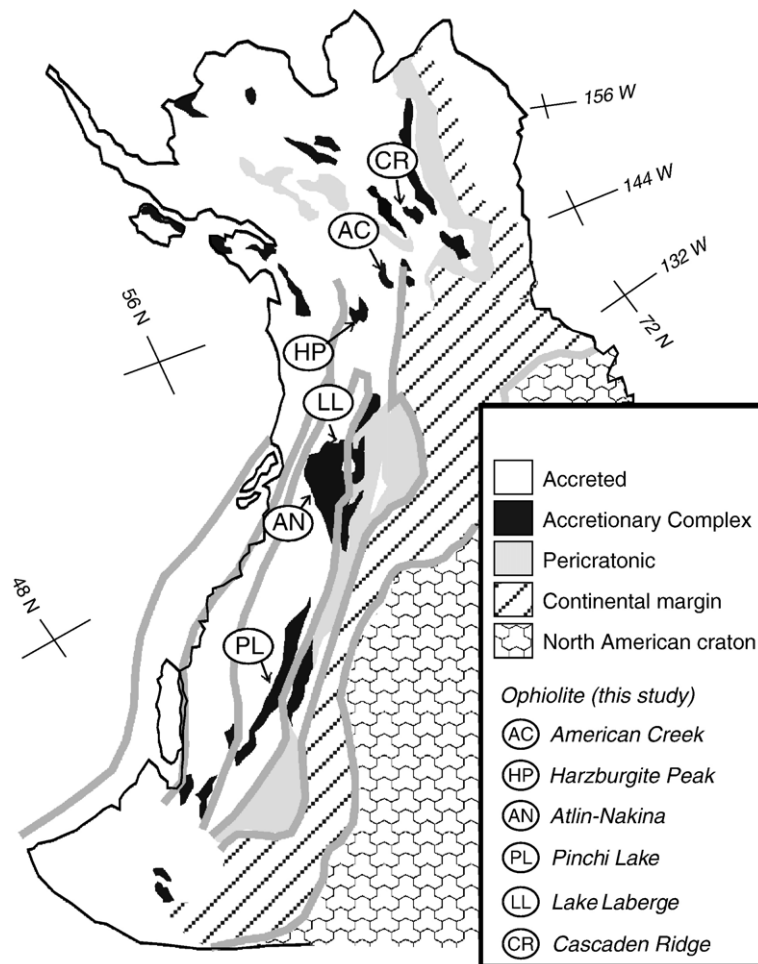


Fig. 1. Simplified geologic map of the northern Cordillera (after [59]) showing the location of major ophiolites sampled for this study. Grey lines separate the major morpho-geologic belts.

serpentinized spinel harzburgite. The age and geologic setting of the ultramafic body is not well constrained; these rocks are in contact with the Jurassic Laberge Group sediments, and may belong to serpentinized harzburgites exposed in the Mississippian–Permian Cache Creek terrane ophiolite further south in Yukon and British Columbia.

2.5. Atlin–Nakina and Pinchi Lake

Ophiolite dominantly of mantle harzburgite tectonite, serpentinite mélange, minor gabbro and volcanics occurs along a northwest trend in the Cache Creek Terrane [29]. Intrusions in the ophiolite have Permian crystallization ages [24]. Superb exposures of mantle tectonite occur in a series of massifs from northwest to southeast: Atlin (Monarch Mountain), Hard Luck Peaks, Peridotite Peak,

Nahlin Mountain and farther south adjacent to Pinchi Lake [30–32].

Peridotites in all the localities are coarse or porphyroclastic harzburgite characterized by coarse olivine, orthopyroxene commonly with exsolution lamellae of clinopyroxene, holly-leaf textured spinel and rare clinopyroxene. States of preservation vary from nearly 100% fresh (Peridotite Peak) to complete serpentinization of olivine (Cascaden Ridge, Lake Laberge). Spinel is always fresh, and thin ‘ferritchromit’ rims developed on spinel in heavily serpentinized samples were avoided in all microbeam studies. The massifs show layering common to many ophiolite mantle sections [33]. Discordant dunite bodies are common in all massifs except Harzburgite Peak. Sampling was done so as to investigate the T, f_{O_2} and bulk chemical variations at different scales (meters to kilometers) within and between massifs.

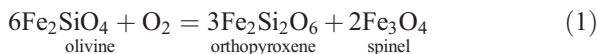
3. Methods

3.1. Geothermometry and oxygen barometry

One goal was to investigate in a statistically robust fashion the T and fO_2 recorded thermobarometrically by spinel within and between peridotite samples and to examine whether this was a function of cooling history, or bulk composition. To do so, requires large numbers of analyses of spinel with a range of grain sizes, presuming smaller grain sizes will close to chemical exchange at lower temperature for a given cooling rate [34]. Spinel is in minor abundance in mantle peridotites (<3–5%) and thus is not statistically well-sampled in standard thin sections. For this reason, the silicate portion in cm-sized pieces (~3 g) of peridotite samples were dissolved in HF acid for 24 h. Spinel grains remaining from this process with a range of diameters (0.1 to 1.2 mm) were hand-picked under a binocular microscope, mounted in epoxy and polished. The diameter of each grain was measured on polished sections using a microscope reticle.

Between 15 and 50 spinel grains from each of 17 peridotite samples were analysed for their major elements using a Cameca SX50 electron microprobe (EMP) at the University of British Columbia (UBC). Operating conditions were 15.0 kV acceleration voltage and a beam current of 20.1 nA. Analytical conditions were 20 s counting time on peaks for major elements, 60 s for Ni and 80 s for V (Table 1 in Appendix A). Natural and synthetic standards were used for calibration. Data reduction was done with the $\varphi(\rho Z)$ method and Fe^{3+} and Fe^{2+} in spinels were calculated assuming perfect stoichiometry [35].

For olivine–spinel assemblages the $FeMg_{-1}$ exchange was used as a geothermometer and the reaction:



was used as an oxygen barometer [36–38]. Olivine and orthopyroxene were not analysed in most samples. The X_{Fe} ($Fe/(Fe+Mg)$) of the coexisting olivine and orthopyroxene was assumed to be identical of that of the whole rock, as shown previously for peridotite (e.g. [39]) and confirmed by olivine and orthopyroxene analyses for eight samples in this study from Harzburgite Peak and Atlin–Nakina. Because many of the samples equilibrated at temperatures below the experimental calibration of Ballhaus et al. we report results from the oxybarometer of Wood [37], which is based on thermodynamic properties of spinels and should extrapolate to lower temperature with more confidence. Nonetheless, both methods [37,38] give results within

0.3 log units of one another for all samples. Temperatures are reported at an assumed pressure of 0.5 GPa, slightly above that below oceanic crust with a typical thickness (~8 km) but the olivine–spinel $FeMg$ thermometer has only a weak pressure dependence (30 °C/GPa). Accuracy and precision for the $Fe^{3+}/\Sigma Fe$ in spinels calculated from EMP data was tested using 10 secondary spinel standards with Fe^{3+} determined by Mössbauer spectroscopy [10,40,41] (Table 2 in Appendix A). The uncertainties in the $Fe^{3+}/\Sigma Fe$ of spinels result in errors of ± 30 °C and ± 0.8 log units in absolute T and fO_2 , respectively, within the uncertainties of the thermometer and oxybarometer. Samples repeatedly analyzed over a three year period gave identical results (± 20 °C, ± 0.3 log units) demonstrating the high precision of the UBC EMP method [42].

3.2. Bulk rock geochemistry

Samples weighing ~0.5 kg were trimmed of all surface alteration with a rock saw and crushed to powders in a disk mill. Major elements, Sc, V, Ni, Cr and Co were determined for 84 samples by X-ray fluorescence (XRF) at McGill University, Montreal or St. Mary's University, Halifax. Sulfur in selected samples was determined by the LECO™ method at McGill University. Trace elements were determined in a subset of 52 samples by solution nebulisation inductively coupled plasma mass spectrometry (ICPMS) at the University of Victoria following the methods of [43]. 200 mg of powdered sample was dissolved in HF–HNO₃ solution in sealed Teflon vessels on a hotplate for 24 h, and dried down. Any remaining residue was attacked with nitric acid, dried down and brought up to 50 mL solution in 5% nitric solution. Solutions were run on a VG2S+ quadrupole ICPMS. One sample analysed repeatedly over the course of 2 yrs produced results within 10%. Some samples were also run using the same ICPMS methods at the University of Saskatchewan to test for interlaboratory consistency. Analytical details are given in Table 2 in Appendix A. Some of the V and Sc data appear in the database used by Lee et al [17] without sulfur, major elements or thermobarometric fO_2 , which are mainly the subject in this study.

4. Results

4.1. Temperature history and thermobarometric fO_2

Spinel from the ophiolite peridotites record a range of Fe–Mg temperatures from 850 to 600 °C. Massifs at Harzburgite Peak and Hard Luck Peak record the highest

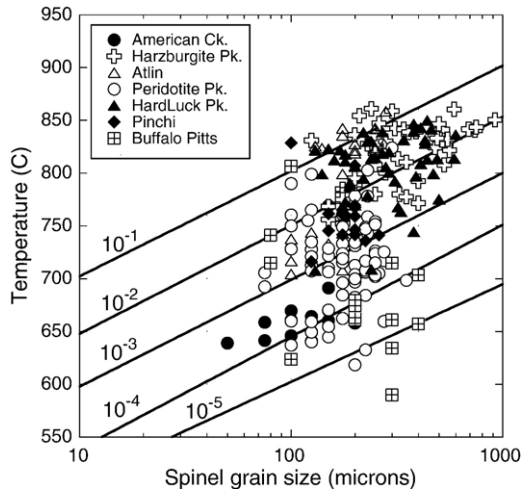


Fig. 2. Plot showing olivine–spinel FeMg_{-1} exchange temperature for different grain sizes of spinels in different ophiolite massifs. Lines show cooling rates (in $^{\circ}\text{C}/\text{yr}$) from diagrams of Ozawa [44]. Data for Buffalo Pitts orogenic peridotite are from [55], all other data from this study.

temperatures (850–750 $^{\circ}\text{C}$). Peridotite Peak records a wide range of temperatures and American Creek records consistently low temperatures (<700 $^{\circ}\text{C}$). The differences in temperatures between massifs are independent of grain size (Fig. 2), whereas within some massifs the temperatures show a correlation with grain size.

The grain size dependence of Fe–Mg temperatures recorded by spinel can be used as a geospeedometer to estimate cooling rates of olivine–spinel assemblages [44]. Recent measurements of the Fe–Mg diffusion kinetics of Fe^{2+} and Mg in aluminous spinel show Ozawa's [44] curves are likely correct for spinels with $\text{Cr}\# < 0.5$ [45]. The $\text{Cr}\#$ ($\text{Cr}/\text{Cr}+\text{Al}$) of spinels from Cordilleran ophiolites in this study vary from 0.2 to 0.75 but show no relationship with temperature between massifs. Using Ozawa's numerical simulations of cooling rates for spinels with a $\text{Cr}\#$ of 0.5 and an initial temperature of 1000 $^{\circ}\text{C}$, the cooling rates of mantle lithosphere in the Cordilleran ophiolites range from 10^{-1} to 10^{-3} $^{\circ}\text{C}/\text{yr}$ for Harzburgite Peak, Hard Luck Peak and Pinchi, to less than 10^{-3} $^{\circ}\text{C}/\text{yr}$ for American Creek and Peridotite Peak. Both Atlin and Peridotite Peak show a wide range of cooling rates, possibly related to structures along which the peridotites were exhumed or exposed shortly after formation (Fig. 2).

The cooling rates recorded by spinel should be regarded as maxima for two reasons. Firstly, revisions to Fe–Mg diffusion coefficients in olivine [46], which are lower than in spinel, indicates the curves could overestimate cooling rates by one or two orders of magnitude

[45]. Secondly, it was assumed that the maximum grain diameter of the spinels was intersected during polishing of the grain mounts. In the likely case that not all spinel grains were intersected at their maximum diameter during polishing, then the points in Fig. 2 would be shifted to the right, implying lower cooling rates. The lower estimates of cooling rates are within the range estimated for lowermost oceanic crust from the Oman ophiolite, based on Ca exchange between olivine and clinopyroxene in gabbros or from cooling half space models for oceanic lithosphere [47,48]. Revised estimates for lowermost crust in the Oman ophiolite, based on new measurements for Ca diffusion in olivine [49] are constrained to about 10^{-4} $^{\circ}\text{C}/\text{yr}$ (L. Coogan, pers. comm. 2005). Nonetheless, the different grain size dependence of T estimates for different massifs suggest they underwent different cooling histories, though the absolute value of the cooling rate is at present uncertain.

Oxygen fugacities recorded thermobarometrically by spinel vary from $\sim \text{NNO}+1$ at American Creek, to $\sim \text{NNO}-2$ at Atlin. Most massifs, however, cluster within 1 $\log f_{\text{O}_2}$ unit between NNO and $\text{NNO}-1$ and exhibit no grain size or T dependence with this variable (Figs. 2, 3, Table 1 in Appendix A).

Many samples are serpentinized to varying degrees, but care was taken to avoid spinel grains that have altered to 'ferritchromit' or magnetite as a result of this process. Furthermore, serpentinization proceeds at temperatures (<400 $^{\circ}\text{C}$) well below those at which primary spinel could reasonably be expected to alter its ferric/ferrous ratio according to reaction Eq. (1). Our samples

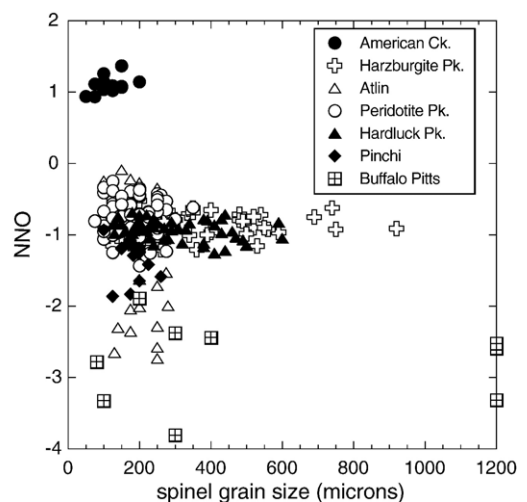


Fig. 3. Plot showing the $\log f_{\text{O}_2}$ recorded by olivine–orthopyroxene–spinel assemblages relative to nickel–bunsenite buffer (NNO) versus grain sizes of spinels in different ophiolite massifs. Data for Buffalo Pitts orogenic peridotite are from [55], all other data from this study.

show no correlation of thermobarometric fO_2 with alteration indices such as LOI (Fig. 4).

4.2. Geochemistry

In order to accurately constrain and examine the paleo fO_2 both within and between ophiolite mantle massifs we used V/Sc systematics. The quality and consistency of analytical data is critical to the use of V/Sc ratios as a fO_2 proxy. For this reason, we compared V and Sc data using ICPMS method between laboratories. Furthermore, as most data in the literature for peridotites is collected using XRF [17,50] we also wished to compare interlaboratory consistency between ICP and XRF data for these key elements.

Our results show that the V/Sc of seven duplicate samples are within 3 to 10% between the Saskatchewan and Victoria ICPMS labs, and two samples run in the Victoria lab are within 1% (Table 2 in Appendix A). Comparison of ICPMS with XRF results shows significant differences. ICPMS produces higher V contents and a more restricted range of Sc, leading to a narrower range of V/Sc compared to XRF (Fig. 5). In addition, the array of V/Sc as a function of depletion as determined by XRF gives a more scattered and opposite trend than ICPMS (Fig. 6A). With ICPMS data, intra- and inter-massif variability is small and the samples from all ophiolites form a tight cluster of V/Sc mostly between 3 and 5 (Fig. 6B). In the remainder of this paper, we use

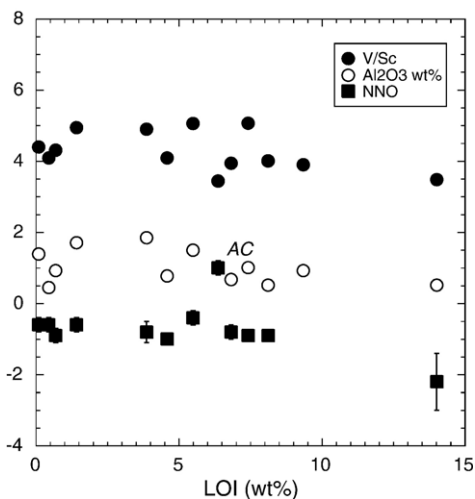


Fig. 4. Plot showing the degree of serpentinization, measured using loss on ignition (LOI) versus Al, V/Sc and thermobarometric fO_2 (relative to nickel–bunsenite buffer (NNO)) for samples from this study. Uncertainties in thermobarometric fO_2 plotted at 1 σ confidence level. Sample from American Creek labelled AC.

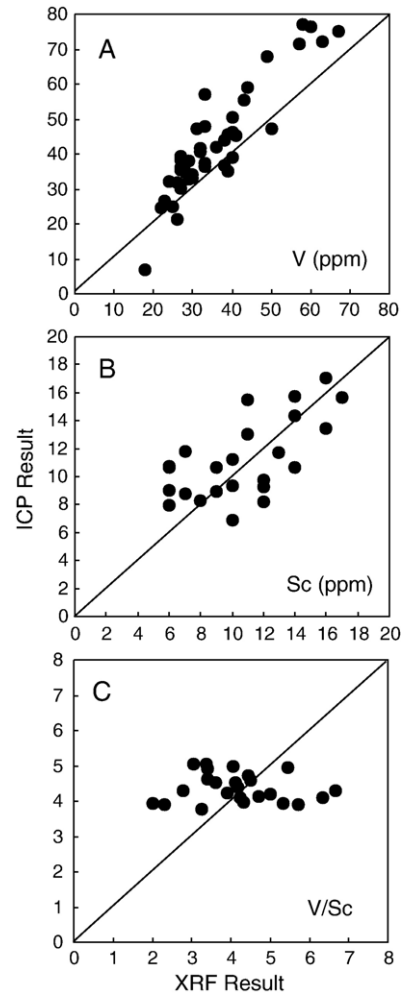


Fig. 5. Comparison of V, Sc and V/Sc for peridotites from this study determined by XRF and ICPMS methods.

and apply the more precise V and Sc contents from ICPMS analysis. Serpentinization (as measured by loss on ignition) also shows no correlation with V/Sc (Fig. 4).

The level of depletion in the ophiolite peridotites is evaluated using Al_2O_3 , because it is insensitive to serpentinization or seafloor weathering [51,52]. All the ophiolite peridotites from this study are depleted, containing less than 2% Al_2O_3 (average of 1.3 wt.%) typical of most other peridotites from ophiolites, modern ocean floor, fore-arcs or intraplate oceanic mantle [50]. Whole rock Al_2O_3 does not depend on the degree of serpentinization, and shows a good correlation with MgO, V and Sc, and the proportion of V partitioned into spinel relative to the whole rock (Fig. 7A,B). CaO is more prone to mobilization during serpentinization [51] explaining some scatter in a few samples from depletion trends with Al_2O_3 (Fig. 7C).

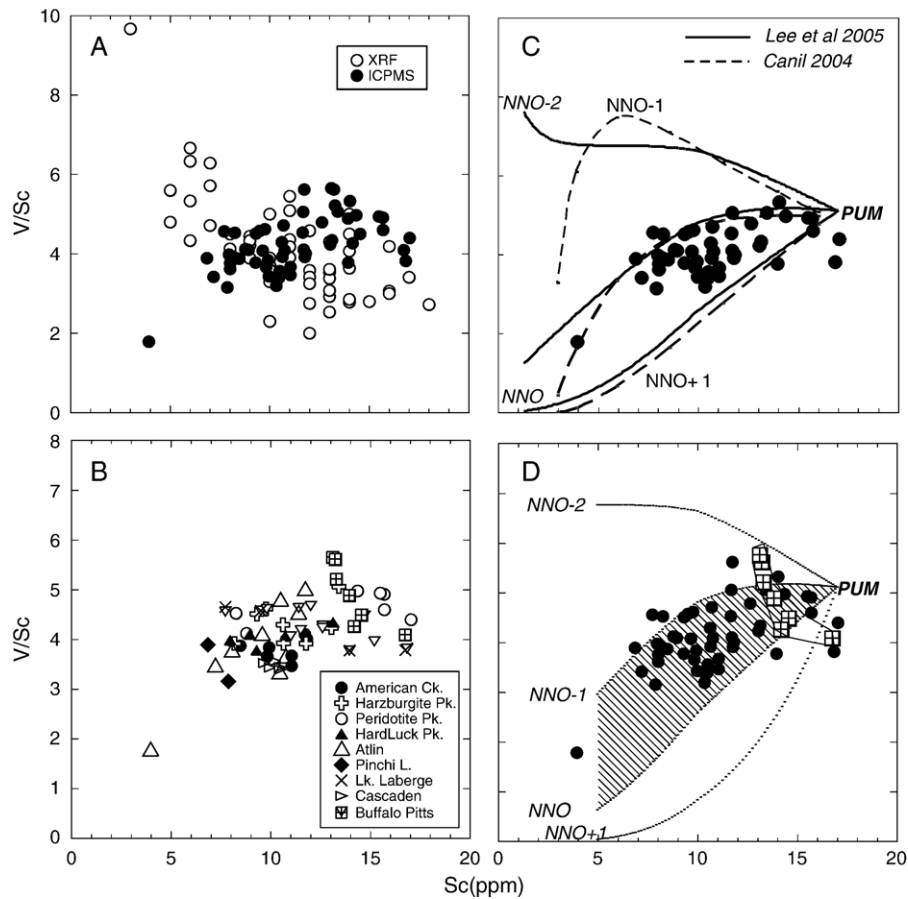


Fig. 6. Plot showing the variation in V/Sc with depletion (Sc) for peridotites from this study. A. Comparison of trends using ICPMS and XRF data, B. all ICPMS data plotted according to individual massifs, C. all massifs shown together compared with trends for residues produced by fractional partial melting at 1.5 GPa at different $\log f_{\text{O}_2}$'s (shown relative to nickel–bunsenite buffer (NNO)) using the model of Lee et al [17] (solid line) and Canil [50]. D. All massifs shown together compared with trends for residues produced by fractional partial melting at 1.5 GPa at different $\log f_{\text{O}_2}$'s using the model of Lee et al (shown relative to nickel–bunsenite buffer (NNO)). Note the V/Sc of most peridotites fall within a narrow range of f_{O_2} (hatched field) during melting (NNO to NNO–1). The residue trends in C. and D. were calculated using the assumed PUM starting material containing 17 ppm Sc and 82 ppm V. Data for Buffalo Pitts orogenic peridotite are from [55].

There is no correlation of depletion with thermobarometric f_{O_2} (Fig. 7D).

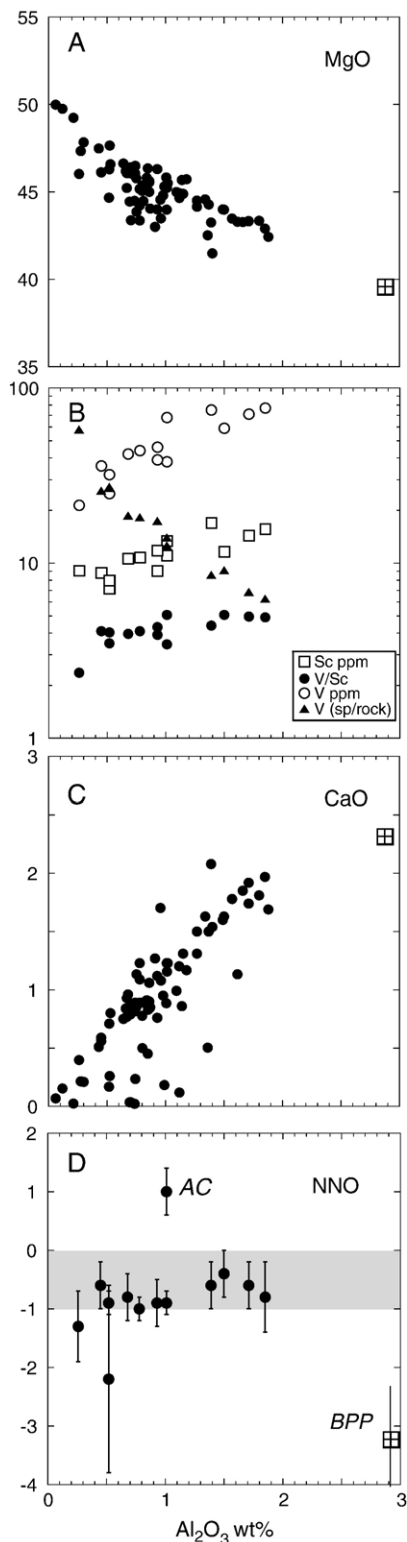
5. Discussion

5.1. The f_{O_2} record during the formation of mantle lithosphere

A plot of Sc versus V/Sc shows that Cordilleran ophiolite peridotites with varying levels of depletion from all locations cluster within a remarkably narrow range of V/Sc (Fig. 6B). The array of V/Sc ratios can be used to estimate the paleo f_{O_2} of these peridotites during formation, by comparison with fractional melting trends calculated as a function of f_{O_2} using partition coefficients (D) for V and Sc between olivine, ortho-

pyroxene, clinopyroxene, spinel and melt [17,50]. These calculations assume that the peridotites formed as residues mostly in the spinel peridotite stability field, as expected for most ophiolites.

The melting model of Lee et al [17] uses peridotite melting reaction stoichiometries from the pMELTS algorithm [53] and shows that the V/Sc in the ophiolite peridotites are consistent with melting at conditions of NNO to NNO–1 (note the Quartz–Fayalite–Magnetite ‘QFM’ buffer is within 0.1 $\log f_{\text{O}_2}$ units of NNO at P – T conditions near the mantle solidus). The model of Canil [12,50], uses experimentally-derived peridotite melting reaction stoichiometries, and produces similar residue trends, but shifted by about 1 $\log f_{\text{O}_2}$ unit higher (Fig. 6C). As both partial melting models use the same D_V values [12], the difference in results is mainly attributable



to choices for D_{Sc} . The Canil model [50] uses the lowest D_{Sc} for olivine, orthopyroxene and clinopyroxene from experiments on mafic/ultramafic systems whereas the Lee et al [17] version uses empirical parameterizations of D_{Sc} for olivine and orthopyroxene and ‘average’ values for clinopyroxene from one experimental study. This comparison shows that the V/Sc systematics in peridotites can be modeled to no better than 1 log $f\text{O}_2$ unit (Fig. 6C) until Sc partitioning in mantle phases is better constrained by new experiments.

Limitations on the knowledge of the exact starting composition are common to all inverse petrologic models, and also affect the absolute $f\text{O}_2$ conditions depicted by the V/Sc array for the peridotites (Fig. 6C,D). Use of a starting material with lower V/Sc than primitive upper mantle (PUM) would place the ophiolite peridotites along an array consistent with more reducing paleo $f\text{O}_2$ conditions during formation. Furthermore, if XRF data for V and Sc were used in the modeling, a more reducing $f\text{O}_2$ range during melting could also be interpreted from the data (Fig. 6A,C). Because of the large scatter in published XRF data for V/Sc on peridotites, and inability to properly evaluate interlaboratory accuracy [15], the ICP methods are deemed a more confident measure of V/Sc for use in paleo $f\text{O}_2$ estimates. Regardless of different starting source compositions, or the use of XRF data, or the application of different melting models, the range of $f\text{O}_2$'s to produce the V/Sc in the ophiolite residues by partial melting remains restricted to within 1 log $f\text{O}_2$ unit.

The use of V abundances as a proxy for $f\text{O}_2$ has been cautioned on the basis that that metasomatism may have overprinted the redox signal encoded in this element [10,54]. It should be noted that V and Sc are moderately (not highly) incompatible elements, and both empirical evidence from metasomatically veined mantle in outcrop, and model calculations, show their abundances are not sufficiently disturbed to affect the outcome of the V/Sc ratio [50]. Metasomatism also cannot explain the narrow range in V/Sc for mantle residues from a variety of ages and geologic settings.

The relationship between paleo- and thermobarometric $f\text{O}_2$ is made more clear by comparing these two parameters in rocks for which both were measured. Because paleo $f\text{O}_2$ modelling uses whole rock V and Sc,

Fig. 7. Correlation of depletion (Al_2O_3) in ophiolite peridotites with A. MgO, B. V, Sc, V/Sc, and the proportion of V in spinel (measured by EMP) relative to whole rock, C. CaO and D. thermobarometric $f\text{O}_2$ for ophiolite peridotites from this study. In D. the uncertainties are given at 2 σ confidence, and the shaded region represents the range of paleo $f\text{O}_2$ derived from V/Sc systematics (Fig. 6D). Sample from American Creek labelled AC. Data for Buffalo Pitts orogenic peridotite (BPP) are from [55].

we averaged the data from spinels from each sample to reflect whole rock thermobarometric fO_2 in this comparison. With the exception of two samples, the narrow range of paleo fO_2 recorded by V/Sc is reflected by an equally narrow range in thermobarometric fO_2 (Figs. 3, 6D), both within and between different ophiolite massifs.

To further test the compatibility of the V/Sc results with thermobarometric fO_2 , we examined an example of continental mantle from an orogenic peridotite massif (Buffalo Pitts) for which V and Sc is measured in the same ICP laboratory, and for which, compared to the ophiolite peridotites, had a longer history and more complex emplacement [55]. Despite its continental mantle affinity, a less depleted composition and a more protracted emplacement history into the crust, the V/Sc ratio (and paleo fO_2) of the Buffalo Pitts massif is equally narrow, but its trend with depletion (Sc) is unlike that for the ophiolite peridotites, showing a negative slope, requiring a lower fO_2 during melting according to the melting models (Fig. 6B,D). Interestingly, the thermobarometric fO_2 for this continental mantle massif is also lower (NNO–2 to NNO–4, Figs. 2, 3) than the ophiolite peridotites, somewhat reflective of its different array in the V/Sc diagram (Fig. 6).

For the relatively young ophiolite peridotites with simple cooling histories, the thermobarometric fO_2 are representative of that attendant during the formation of a residue recorded by V/Sc. In contrast, the results for the Buffalo Pitts massif show that for ancient continental mantle, the thermobarometric fO_2 is not necessarily reflective of the fO_2 during their formation. This case explains the surprisingly narrow range in V/Sc observed for numerous continental mantle xenoliths from diverse settings and having a range of thermobarometric fO_2 's of almost 5 log units [17]. In continental mantle, with a longer-lived history, the thermobarometric fO_2 record is an ambiguous, and most likely fallacious measure of the fO_2 attendant during melting to form a residue.

5.2. Oxygen behaviour during partial melting

The majority of ophiolite samples show no correlation of thermobarometric or paleo fO_2 with depletion (Fig. 6D). This requires that fO_2 (relative to a solid buffer) remain constant during partial melting. A similar relationship of constant relative fO_2 is well known for lavas along a liquid line of descent [56] and has been interpreted to mean that the system was open to oxygen during crystallization and differentiation [57,58]. It appears mantle residues can behave in a similar manner, and 'breathe' in order to maintain a constant relative fO_2 during partial melting to produce a residue.

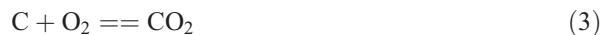
One possibility is that an incompatible element with a capacity to control the O budget during the partial melting process modulates the ambient fO_2 in the residues recorded thermobarometrically or by whole rock V/Sc. Ferric iron, sulfur, hydrogen and carbon are all incompatible during melting, and each can potentially act as internal oxygen buffers [7–9]. Some constraints on the interrelationship of these elements and mantle fO_2 can be offered using samples in this study with their simple depletion and cooling history.

Whole rock FeO and Fe_2O_3 were not determined as part of this study because many of the rocks are serpentinized, and wet chemical analyses of whole rock $Fe^{3+}/\Sigma Fe$ in peridotites is fraught with uncertainty [9]. The Fe_2O_3 content of the ophiolite peridotites was instead estimated using the correlation of Fe_2O_3 with Al_2O_3 in a variety of mantle peridotites [9], which gives the relationship:

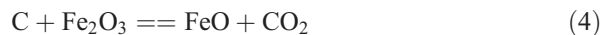
$$wt.\%Fe_2O_3 = 0.092 \cdot wt\%Al_2O_3 + 0.043 \quad (2)$$

This equation reproduces the measured Fe_2O_3 contents of all but one peridotite sample in [9] to within 20%, which we assume here as an uncertainty. Application of Eq. (2) to the ophiolite peridotites from this study show that they are impoverished in Fe_2O_3 (containing 0.05–0.2 wt.%). This would seem to rule out Fe^{3+}/Fe^{2+} as being a major control on ambient fO_2 during melting, but rather that it is controlled by another redox couple.

Almost all ophiolite residues from this study lie along the CCO buffer:



at their assumed P of origin (0.5 GPa) (Fig. 8). This observation is true of many mantle peridotites, and attests to strong control by carbon–fluid equilibria in regulating fO_2 during the melting process [8]. The presence of graphite may control the ferric–ferrous ratios of the residue:



which ultimately governs the thermobarometric fO_2 recorded by Eq. (1) in mantle lithosphere after it forms.

The abundance and therefore buffering capacity of C in the mantle is uncertain [9], but the calculations of Holloway [1] show that only a small amount of C (40 to 80 ppm) is required to maintain a graphite-saturated MORB source region, and thereby control melt CO_2 content, and the Fe^{3+}/Fe^{2+} and fO_2 of melt and residue

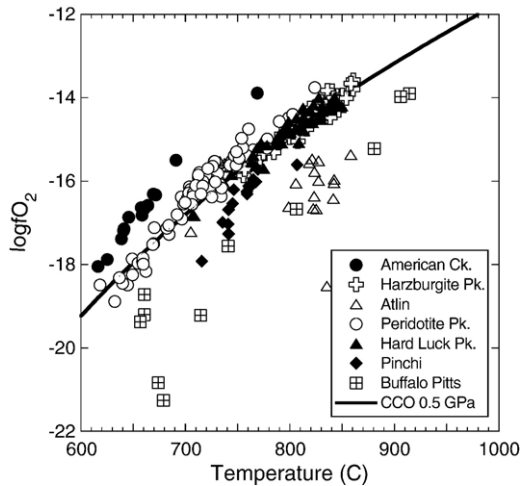


Fig. 8. Thermobarometric fO_2 recorded by all spinels plotted against olivine–spinel Fe–Mg temperature for all ophiolite samples from this study and the Buffalo Pitts orogenic mantle massif [55]. Error bars on thermobarometric fO_2 are 0.5 log units based on precision of multiple analyses. Also shown for reference is the CCO buffer [60] calculated at 0.5 GPa, the assumed pressure of origin of the ophiolite residues.

during partial melting. Holloway's [1] calculations are not sensitive to the presence of H_2O in the mantle, and for graphite-saturated melting in a system closed to oxygen, show a change of about 2 log fO_2 units (NNO–0.5 to NNO–2.5) with up to 15% partial melting to produce basalt. In contrast, we observe almost no variation of either paleo- or thermobarometric fO_2 with depletion for residues from this study (Figs. 3, 6, 7). Note however that the ophiolite residues from this study are products of more advanced degrees of melting than modeled in Holloway's calculations. For example, the Al_2O_3 content of the ophiolite peridotites are all less than 2 wt.%, suggesting they are products of greater than 15–25%, or greater than 20% partial melting, according to either the Canil [50] or Lee et al [17] melting models, respectively. Holloway's calculations show that relative fO_2 , the Fe^{3+}/Fe^{2+} and C content of the melt (and residue) change little after 10% melting, explaining the invariance of fO_2 with depletion at such high degrees of melting. Nonetheless, this does not explain why the ophiolite residues maintained a constant and high fO_2 (i.e. near NNO–1), unless the system were open to oxygen.

This observation can be taken to imply that carbon controls the Fe^{3+}/Fe^{2+} of mantle residues according to Eq. (4) but is not buffering mantle fO_2 , meaning the melt–residue system is open to oxygen. A similar conclusion was reached by Bezos and Humler [11] based on the nearly constant $Fe^{3+}/\Sigma Fe$ for over 100 MORB glasses which they interpret to have been produced by a range of degrees of partial melting. Further tests of this idea

require more quantitative data on the partitioning of ferric iron between melt and residue in the presence of carbon in controlled melting experiments, or the examination of Fe^{3+}/Fe^{2+} and fO_2 in ophiolite residues with simple histories but which have experienced less degree of depletion than those studied here. Unfortunately, such experiments have been difficult to accomplish so far, and less depleted peridotites in ophiolites are rare [50].

Two samples do not plot along the CCO buffer at the assumed P of origin of the ophiolite residues (0.5 GPa). The sample from American Creek requires a much higher P of equilibration (1.5 GPa) to lie along CCO (Fig. 8). Such a high pressure of formation is unlikely for mantle lithosphere from an ophiolite. This sample stands outside of the trends of thermobarometric fO_2 with degree of depletion, suggesting this massif may simply represent a residue whose interplay of Fe and C (via Eqs. (2), (3) or (4)) has not been controlled by partial melting in the presence of graphite. A second sample off the CCO trend is from Atlin, and gives lower thermobarometric fO_2 compared to other samples from the same massif (Fig. 8). Suspiciously, this sample plots along a same fO_2 trend as samples from the Buffalo Pitts continental mantle massif with a protracted cooling history. These two outliers show that even in young mantle with a relatively simple geologic history, complications may arise that obscure the signal recorded by thermobarometric fO_2 . The latter may not necessarily always provide a robust record of the fO_2 during partial melting to form a residue. For these reasons, interpretation of mantle fO_2 at its time of formation, or of the behaviour of oxygen during the partial melting process, should not be based solely on thermobarometric fO_2 recorded in continental mantle samples.

Acknowledgements

We thank C. Charnell, L. Ferreira, and R. Rhodes for their lab assistance, and L. Coogan for his idea on spinel separations, and an informal review. G. Shelnut made the sample collections in Alaska and near Pinchi Lake. M. Raudsepp and J. Spence are thanked for their assistance with EMP and ICPMS analyses. We appreciate reviews by D. Francis, B. Wood and R. Carlson. This research was supported by funds from Yukon Geological Survey, British Columbia Ministry of Energy and Mines and NSERC of Canada to DC.

Appendix A. Supplementary data

Supplementary data associated with this article can be found, in the online version, at [doi:10.1016/j.epsl.2006.04.038](https://doi.org/10.1016/j.epsl.2006.04.038).

References

- [1] J.R. Holloway, Graphite-melt equilibria during mantle melting: constraints on CO₂ in MORB magmas and the carbon content of the mantle, *Chem. Geol.* 147 (1998) 89–97.
- [2] R.W. Luth, Carbon and carbonates in the mantle, *Mantle Petrology: Field observations and High Pressure Experimentation*, in: Y. Fei, C.M. Bertak, B.O. Mysen (Eds.), *Spec. Publ.*, vol. 6, The Geochemical Society, 1999, pp. 297–316.
- [3] J.E. Mungall, Roasting the mantle: slab melting and the genesis of major Au and Au-rich deposits, *Geology* 30 (2002) 915–918.
- [4] H.D. Holland, *The Chemistry of the Atmosphere and Oceans*, Wiley Interscience, New York, 1978.
- [5] J.F. Kasting, D. Catling, Evolution of a habitable planet, *Annu. Rev. Astron. Astrophys.* 41 (2003) 429–463.
- [6] B.J. Wood, L.T. Bryndzia, K.E. Johnson, Mantle oxidation state and its relationship to tectonic environment and fluid speciation, *Science* 248 (1990) 337–345.
- [7] C. Ballhaus, R.F. Berry, D.H. Green, Oxygen fugacity controls in the earth's upper mantle, *Nature* 348 (1990) 437–440.
- [8] J. Blundy, J. Brodholt, B.J. Wood, Carbon fluid equilibria and the oxidation state of the upper mantle, *Nature* 349 (1991) 321–324.
- [9] D. Canil, H.S.C. O'Neill, D.G. Pearson, R.L. Rudnick, W.F. McDonough, D.A. Carswell, Ferric iron in peridotites and mantle oxidation states, *Earth Planet. Sci. Lett.* 123 (1994) 205–220.
- [10] C. McCammon, M. Kopylova, A redox profile of the Slave mantle and oxygen fugacity control in the cratonic mantle, *Contrib. Mineral. Petrol.* 148 (2004) 55–68.
- [11] A. Bezos, E. Humler, The Fe³⁺/ΣFe ratios of MORB glasses and their implications for mantle melting, *Geochim. Cosmochim. Acta* 69 (3) (2005) 711–725.
- [12] D. Canil, Vanadium in peridotites, mantle redox and tectonic environments: Archean to present, *Earth Planet. Sci. Lett.* 195 (2002) 75–90.
- [13] J. Delano, Redox history of the Earth's interior since ~3900 Ma: implications for prebiotic molecules, *Origin Life Evol. Bio.* 31 (2001) 311–341.
- [14] D. Canil, Vanadium partitioning and the oxidation state of Archean komatiite magmas, *Nature* 389 (1997) 842–845.
- [15] C.T.A. Lee, A.D. Brandon, M. Norman, Vanadium as a proxy for paleo-fO₂ during partial melting: prospects, limitations and implications, *Geochim. Cosmochim. Acta* 67 (2003) 3045–3064.
- [16] Z.-X. Li, C.-T.A. Lee, The constancy of upper mantle fO₂ through time inferred from V/Sc ratios in basalts, *Earth Planet. Sci. Lett.* 228 (2004) 483–493.
- [17] C.-T. Lee, W.P. Leeman, D. Canil, Z.A. Li, Similar V/Sc systematics in MORBs and arc basalts: implications for the oxygen fugacities of their mantle source regions, *J. Petrol.* 46 (2005) 2313–2336.
- [18] E.M. Moores, Origin and emplacement of ophiolites, *Rev. Geophys.* 20 (1982) 735–760.
- [19] C.J. Hawkesworth, P.D. Kempton, N.W. Rogers, R.M. Ellam, P.W. van Calsteren, Continental mantle lithosphere, and shallow level enrichment processes in the Earth's mantle, *Earth Planet. Sci. Lett.* 96 (1990) 256–268.
- [20] D.G. Pearson, G.M. Nowell, The continental lithospheric mantle: characteristics and significance as a mantle reservoir, *Philos. Trans. R. Soc. Lond.* 360 (2002) 2382–2410.
- [21] R.G. Coleman, Prospecting for ophiolites along the California continental margin, in: Y. Dilek, E.M. Moores (Eds.), *Ophiolites and Oceanic Crust*, Geological Society of America, Denver, 2000, pp. 351–364.
- [22] J.G. Shellnutt, D. Canil, S.T. Johnston, Preliminary results of a petrological study of ultramafic rocks of the northern Cordillera, *Yukon Geol. Explor.* 2001 (2001) 229–237.
- [23] D. Canil, S.T. Johnston, Harzburgite Peak: a large mantle tectonite in ophiolite from southwestern Yukon, *Yukon Geol. Explor.* 2002-1 (2002) 1–10.
- [24] M.G. Mihalynuk, S.T. Johnston, J.M. English, F. Cordey, M.E. Villeveuve, L. Rui, M.J. Orchard, *Atlin TGI, Part II, Regional Geology and Mineralization of the Nakina Area (NTS 104N/2W and 3)*, Geological Fieldwork 2002 Paper 2003-1, 2003, pp. 9–14.
- [25] J.M. English, S.T. Johnston, Collisional orogenesis in the northern Canadian Cordillera: implications for Cordilleran crustal structure, ophiolite emplacement, continental growth, and the terrane hypothesis, *Earth Planet. Sci. Lett.* 232 (2005) 333–344.
- [26] R.A. Loney, G.R. Himmelberg, Ultramafic rocks of the Livengood terrane, in: J.P. Galloway, T.A. Hamilton (Eds.), *Geologic Studies of Alaska by the US Geological Survey during 1987*, United States Geological Survey Circular, vol. 945, 1988, pp. 46–48.
- [27] H.L. Foster, G.W. Cushing, T.E.C. Keith, Early Mesozoic tectonic history of the Boundary area, east-central Alaska, *Geophys. Res. Lett.* 12 (1985) 553–556.
- [28] C.J.R. Hart, A transect across northern Stikinia: geology of the northern Whitehorse map area, southern Yukon Territory (105D/13–16), *Expl. Geol. Services Div., Indian and Northern Affairs Canada Bulletin*, vol. 8, 1997, 113 pp.
- [29] J.W.H. Monger, Paleozoic rocks of the Atlin Terrane, northwestern British Columbia and south-central Yukon, *Geol. Surv. Can. Paper*, vol. 74–27, 1975.
- [30] C.H. Ash, Origin and tectonic setting of the ophiolitic and related rocks in the Atlin area, British Columbia (NTS 104N), *British Columbia Energy, Mines and Petroleum Resources Bulletin*, vol. 84, 1994, 48 pp.
- [31] M. Mihalynuk, L. Fiererra, S. Robertson, F.A.M. Devine, F. Cordey, Geology and new mineralization in the Joss'alun belt, Atlin area, *Geological Fieldwork 2003 Paper*, vol. 2004-1, 2004, pp. 61–83.
- [32] J.V. Ross, The internal fabric of an alpine peridotite near Pinchi Lake, central British Columbia, *Can. J. Earth Sci.* 14 (1977) 32–44.
- [33] H.J.B. Dick, J.M. Sinton, Compositional layering in Alpine peridotites: evidence for pressure solution creep in the mantle, *J. Geol.* 87 (1979) 403–416.
- [34] M.H. Dodson, Closure profiles in cooling systems, *Mater. Sci. Forum* 7 (1986) 145–154.
- [35] G.T.R. Droop, A general equation for estimating Fe³⁺ concentrations in ferromagnesian silicates and oxides from microprobe analyses, using stoichiometric criteria, *Min. Mag.* 51 (1987) 431–435.
- [36] H. O'Neill, V.J. Wall, The olivine–orthopyroxene–spinel oxygen geobarometer, the nickel precipitation curve, and the oxygen fugacity of the Earth's upper mantle, *J. Petrol.* 28 (1987) 1169–1191.
- [37] B.J. Wood, Oxygen barometry of spinel peridotites, in: D.H. Lindsley (Ed.), *Oxide Minerals: Petrologic and magnetic significance*, Review in Mineralogy, vol. 25, Mineralogical Society of America, Washington, D.C., 1990, pp. 417–432.
- [38] C. Ballhaus, R.F. Berry, D.H. Green, High pressure experimental calibration of the olivine–orthopyroxene–spinel oxygen barometer: implications for the oxidation state of the upper mantle, *Contrib. Mineral. Petrol.* 107 (1991) 27–40.
- [39] F.R. Boyd, Origins of peridotite xenoliths: major element considerations, *Short Course on High P and T Research on the Lithosphere*, U. Siena, Italy, 1997.
- [40] B.J. Wood, D. Virgo, Upper mantle oxidation state: ferric iron contents of ilmenite spinels by 57Fe Mössbauer spectroscopy

- and resultant oxygen fugacities, *Geochim. Cosmochim. Acta* 53 (1989) 1277–1291.
- [41] D. Canil, D. Virgo, C.M. Scarfe, Oxidation states of mantle xenoliths from British Columbia, Canada, *Contrib. Mineral. Petrol.* 104 (1990) 453–562.
- [42] Y. Fedortchouk, D. Canil, J.A. Carlson, Dissolution forms in Lac de Gras diamonds and their relationship to the temperature and redox state of kimberlite magma, *Contrib. Mineral. Petrol.* 150 (2005) 54–69.
- [43] H. Longerich, G. Jenner, S. Jackson, B. Fryer, Inductively coupled plasma-mass spectrometric analysis of geological samples: a critical evaluation based on case studies, *Chem. Geol.* 83 (1990) 105–118.
- [44] K. Ozawa, Olivine–spinel geospeedometry: analysis of diffusion-controlled Mg–Fe²⁺ exchange, *Geochim. Cosmochim. Acta* 48 (1984) 2597–2611.
- [45] H.-P. Liermann, J. Ganguly, Diffusion kinetics of Fe²⁺ and Mg in aluminous spinel: experimental determination and applications, *Geochim. Cosmochim. Acta* 66 (2002) 2903–2913.
- [46] S. Chakraborty, Rates and mechanisms of Fe–Mg interdiffusion in olivine at 980–1300 C, *J. Geophys. Res.* 102 (B6) (1997) 12317–12331.
- [47] L.A. Coogan, G.R.T. Jenkin, R.N. Wilson, Constraining the cooling rate of the lower oceanic crust: a new approach applied to the Oman ophiolite, *Earth Planet. Sci. Lett.* 199 (2002) 127–146.
- [48] J. MacLennan, T. Hulme, S. Singh, Cooling of the lower oceanic crust, *Geology* 33 (2005) 357–360.
- [49] L.A. Coogan, A. Hain, S. Stahl, S. Chakraborty, Experimental determination of the diffusion coefficient for calcium in olivine between 900C and 1500C, *Geochim. Cosmochim. Acta* 69 (2005) 3683–3694.
- [50] D. Canil, Mildly incompatible elements in peridotites and the origins of mantle lithosphere, *Lithos* 77 (2004) 375–393.
- [51] R.G. Coleman, T.E. Keith, A chemical study of serpentinization—Burro Mountain, California, *J. Petrol.* 12 (1971) 311–329.
- [52] J.E. Snow, H.J.B. Dick, Pervasive magnesium loss by marine weathering of peridotite, *Geochim. Cosmochim. Acta* 59 (1995) 4219–4235.
- [53] M.S. Ghiorso, M.M. Hirschmann, P.W. Reiners, V.C. Kress, The pMELTS: a revision of MELTS for improved calculation of phase relations and major element partitioning related to partial melting of the mantle to 3 GPa, *Geochem. Geophys. Geosys.* 3 (2002), doi:10.1029/2001GC000217.
- [54] A.B. Woodland, M. Koch, Variation in oxygen fugacity with depth in the upper mantle beneath the Kaapvaal craton, Southern Africa, *Earth Planet. Sci. Lett.* 214 (2003) 295–310.
- [55] D. Canil, S.T. Johnston, K. Evers, J.G. Shellnutt, R.C. Creaser, Mantle exhumation in an early Paleozoic passive margin, northern Cordillera, Yukon, *J. Geol.* 111 (2003) 313–327.
- [56] I.S.E. Carmichael, The mineralogy of Thingmuli, a Tertiary volcano in eastern Iceland, *Am. Mineral.* 52 (1967) 1815–1841.
- [57] I.S.E. Carmichael, M. Ghiorso, Oxidation–reduction relations in basic magma: a case for homogeneous equilibria, *Earth Planet. Sci. Lett.* 78 (1986) 200–210.
- [58] I.S.E. Carmichael, The redox states of basic and silicic magmas: a reflection of their source regions? *Contrib. Mineral. Petrol.* 106 (1991) 129–141.
- [59] J.W.H. Monger, Plate tectonics and northern Cordilleran geology: an unfinished revolution, *Geosci. Can.* 24 (1997) 189–198.
- [60] D.J. Frost, B.J. Wood, Experimental measurements of the fugacity of CO₂ and graphite/diamond stability from 35 to 77 kbar at 925 to 1650 °C, *Geochim. Cosmochim. Acta* 61 (1997) 1565–1574.